Exploring pottery technology and mineralogical, petrographic and chemical composition at the Neolithic pile-dwelling site of Palù di Livenza in north-east Italy

F. Bernardini[1,2] · M. Velicogna[3] · A. De Min[3] · N. Barago[3] · F. Antonelli[4] · R. Micheli[5] · M. Piorico[6] · S. Roma[6] · P. Visentini[7]

Abstract

Palù di Livenza is a Neolithic pile-dwelling site located in north-east Italy, inscribed since 2011 on the World Heritage List of UNESCO in the transnational serial property "Prehistoric pile-dwellings around the Alps". Its study is crucial for investigating the transition from the Recent to Late Neolithic periods in the region. Eighteen vessels from 5 structural phases, dated approximately between 4300/4200 and 3600 BC, have been analysed using X-ray computed microtomography, X-ray diffraction, inductively coupled plasma optical emission and mass spectrometry, as well as portable X-ray fluorescence (pXRF), in order to investigate the pottery forming techniques, the technology and the provenance of the vessels based on their minero-petrographic and chemical characteristics. The results of pXRF analyses have been further evaluated through principal component analysis (PCA). The results obtained indicate that most of the vessels, including the four-spouted vessels typical of the Square Mouthed Pottery culture, were locally produced using the coiling technique. The vessels were tempered with carbonate material that has dissolved due to taphonomic factors and/or large fragments of other rocks originating form geological formations outcropping nearby the archaeological site. The identified fabric groups, in use throughout the entire duration of the settlement, seem to suggest that no significant technological changes occurred at the transition between Recent and Late Neolithic. Interestingly, the PCA analysis of reliable chemical elements revealed that, despite the overall similarity of the assemblage, certain samples with distinct chronology and typology demonstrate remarkably homogeneous chemical characteristics. This suggests slight variations in the raw materials and/or recipes used over time.

Keywords Pottery · Neolithic · Pile dwelling settlement · North-east Italy · Pottery forming techniques · Technology · Mineralogical-petrographic and chemical characterization

F. Bernardini
fbernard@ictp.it; federico.bernardini@unive.it

[1] Department of Humanistic Studies, Università Ca'Foscari Venezia, Dorsoduro 3484/D, Venezia 30123, Italy

[2] Multidisciplinary Laboratory, The Abdus Salam International Centre for Theoretical Physics, Strada Costiera 11, Trieste 34151, Italy

[3] Department of Mathematics, Informatics and Geosciences, University of Trieste, Via Weiss 8, Trieste 34127, Italy

[4] LAMA - Laboratory for Analysing Materials of Ancient origin, University Iuav of Venice, San Polo 2468/B, Venezia 30125, Italy

[5] Soprintendenza Archeologia, Belle Arti e Paesaggio del Friuli Venezia Giulia, Piazza della Libertà 7, Trieste 34135, Italy

[6] C/O Museo Friulano di Storia Naturale, via C. Gradenigo Sabbadini 24-32, Udine 34100, Italy

[7] Museo Friulano di Storia Naturale, via C. Gradenigo Sabbadini 24-32, Udine 34100, Italy

Introduction and archaeological background

Palù di Livenza, located in north-east Italy, is a significant Neolithic settlement situated in a wetland area near the base of the Cansiglio plateau, where the Livenza river springs originate (Fig. 1a). Although wooden poles and archaeological artefacts have been discovered in the vicinity since the 19th century, it was not until the early 1980s that the site's archaeological importance became evident through initial investigations near a drainage channel within the basin.

Subsequent systematic studies, particularly focused on Sectors 1 and 2 along the drainage channel (Fig. 1b), revealed a wealth of materials from a Neolithic pile dwelling settlement, including wooden structures on elevated platforms and evidence of land reclamation efforts. However, the area under investigation was impacted by modern channel excavation (Corti et al. 1998, 2002; Vitri and Visentini 2002; Vitri et al. 2002), resulting in disturbances to the archaeological deposits and leaving several unresolved issues.

Nevertheless, Palù di Livenza was inscribed on the UNESCO World Heritage List in 2011 as part of the transnational serial property "Prehistoric pile-dwellings around the Alps" due to the abundance and well preservation of archaeological evidence found.

A new phase of research, directed by Soprintendenza Archeologia, Belle Arti e Paesaggio del Friuli Venezia Giulia and conducted between 2013 and 2021 in a previously unexplored area known as Sector 3, provided an untouched archaeological deposit ideal for investigation (Fig. 1b). The aim was to gain deeper insights into Neolithic life, refine chronology, and understand settlement dynamics.

Although the excavation area in Sector 3 was limited to only 50 m^2, it proved to be highly promising, offering a fundamental stratigraphic window into the evolution of the Neolithic pile dwelling settlement (Micheli 2018; Micheli et al. 2017, 2018; Tasca et al. 2019; Bernardini et al. 2023; Zappa et al. 2023).

Numerous wooden components, encompassing both horizontal beams and fixed vertical poles, were meticulously identified. Across the various phases, the foundation systems displayed consistent technical features and architectural schemes. These comprised interlocking and intersecting beams and plinths, crucial for stabilizing the stilt foundations. Notably, these structures served dual purposes, accommodating both residential units and ancillary buildings such as warehouses or granaries. Key structural elements included long sleeping beams featuring quadrangular-shaped through holes placed at regular intervals, supporting the load-bearing poles through the mortise and tenon interlocking system. Moreover, the inclusion of numerous piles, seemingly inserted without a predetermined order,

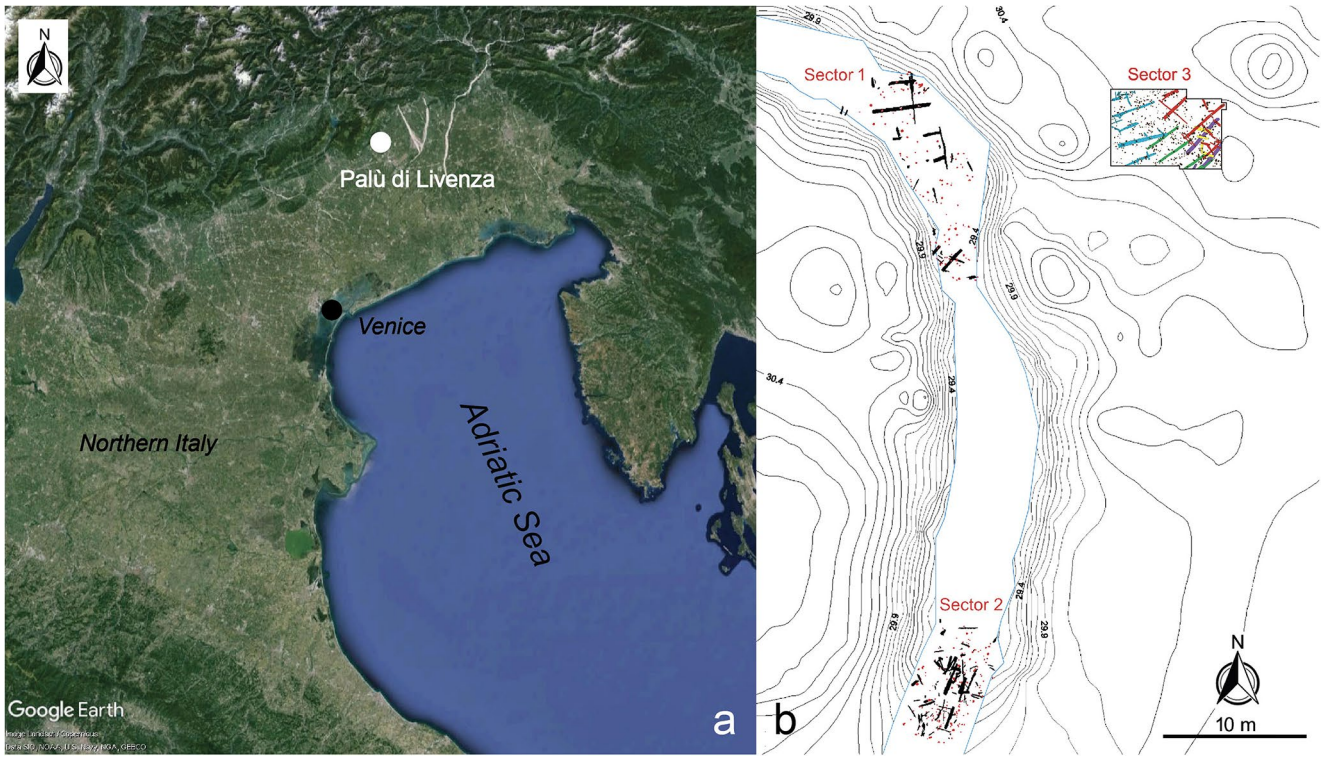

Fig. 1 (**a**): Location of the Neolithic pile dwelling site of Palù di Livenza. (**b**): The artificial channel with the location of Sectors 1–3. DMS geographical coordinates of the archaeological site are: 46° 1'17.49"N; 12°28'55.28"E

further complemented the plinth and beam systems. These elements were integrated concurrently or subsequently to building construction (Micheli et al. 2022, 2023).

The identification of five structural phases within Sector 3 serves as evidence for the existence of at least four successive Neolithic settlements in the central-northern region of the Palù basin. Extensive radiocarbon dating, including numerous unpublished dates, reveals a pattern of Neolithic occupation spanning from approximately 4300/4200 to 3600 cal BC, encompassing both the Recent and Late Neolithic periods. The abundance of ceramics and lithic artefacts collected suggests that the initial four structural phases (1–4) can be attributed to the Square Mouthed Pottery culture (hereafter SMP culture), exhibiting various aspects evolved during the latter centuries of the 5th millennium cal BC. Conversely, the final phase of occupation (phase 5) is distinguished by the presence of materials typical the Late Neolithic Alpine Groups, dating between approximately 3950 and 3650 cal BC (Micheli et al. 2018).

The paper aims to investigate the pottery forming techniques, the technology and the provenance of the investigated vessels based on their minero-petrographic and chemical characteristics, using several destructive and non-destructive techniques. The pottery forming techniques used to produce the four-spouted vessels, typical elements of the SMP culture (Mottes et al. 2011; Visentini 2018), are, in fact, not well known and have never been studied applying advanced imaging techniques such as X-ray computed micro-tomography (microCT). At the same time, the relatively long occupation of Palù di Livenza and the detailed stratigraphic and chronological information available allow us to investigate the evolution of pottery technology during a crucial phase, that is the end of the SMP culture and the advent of earliest Late Neolithic groups in north-east Italy. Currently, only a few sites excavated using modern stratigraphic methods can contribute to reconstruct this complex transition. The interpretative framework of this period has undergone significant changes in recent years, particularly highlighting the distinct evolution of the last style of the SMP culture, known as the "incised and impressed style," documented at Palù di Livenza. This style reflects a specific cultural identity found exclusively in north-east Italy, spanning between the provinces of Mantua and Trento, Veneto, and western Friuli. However, this identity loses its coherence and territoriality during the Late Neolithic period, coinciding with the emergence of new cultural groups that no longer convey unity through symbolic messages, exemplified by distinctive pottery productions. This shift is notably reflected in the Late Neolithic ceramic complex of Palù di Livenza. Such transitional phase in northern Italy, particularly in north-east Italy, is characterized by the gradual dissolution of the SMP culture, the arrival of Northern and Western cultural groups, alongside the emergence of the first metallurgy.

Since pottery technological choices often reflect complex sociocultural factors and their possible evolution through time (Gosselain and Livingstone-Smith 2005; Albero Santacreu 2014; Rice 2015), it is clear that the characterization of the selected Palù pottery vessels goes well beyond the definition of minero-petrographic and chemical groups. It can contribute in understanding the changes occurred between Recent and Late Neolithic in north-east Italy.

Finally, our analysis aims to determine whether the pottery was locally produced or if at least some vessels, typologically comparable with types in use in other areas during the same time, were locally produced or imported.

Materials

The excavations in Sector 3 of the prehistoric site have been continuous and systematic, resulting in the recovery of a large quantity of pottery artefacts. These findings have significant diagnostic value for reconstructing the chronological and cultural phases of the settlement's development. Detailed stratigraphic information, particularly related to the identified structural phases (Phase 1–5), along with a considerable number of radiometric dates, enhances their potential. It's important to note that the ongoing study of Palù di Livenza presents a unique opportunity to shed light on various chronological and cultural aspects of north-east Italy during Recent and Late Neolithic. For this reason, the Friulian Museum of Natural History in Udine has undertaken a thorough investigation of the pottery assemblage, encompassing both quantitative (counting and weighing of finds distinguished between diagnostic and non-diagnostic elements) and qualitative data (definition of pottery paste types; typological classification of finds). This endeavour is complemented by the creation of a digital archive and the documentation of selected diagnostic finds through drawings and photographs.

In total, approximately 30,200 pottery items were processed, among which 4,530 are diagnostic items, including single finds or reassembled pots (from 2 or more fragments), at present only partially studied. The pottery materials were categorized based on two main criteria: artefact type and paste type. Paste types were identified through direct observation of key macroscopic features (i.e. inclusions: grain size and shape; sorting of the grains; porosity) resulting in the identification of 21 pottery paste types.

18 pottery finds (Table 1; Figs. S1-S4) were selected for archaeometric analysis to obtain information on production technology, the minero-petrographic and chemical characteristics of the pottery pastes. The sampling primarily

Table 1 The materials selected for analysis with an indication of the analyses performed, the weight of the samples taken, the macroscopic definition of the pastes, the archaeological phases they belong to and the numbers assigned at the Friulian Museum of Natural History

Labels	Museum number	Phase	Pastes	Weight (gr)	methods
PAL1	2	5B	S	2,2	microCT; OM; XRD; ICP-OES/MS; pXRF
PAL2	15	5 A	R	-	microCT; pXRF
PAL3	20	4	C	2,06	microCT; OM; XRD; ICP-OES/MS; pXRF
PAL4	1	1	R	5,5	microCT; OM; XRD; ICP-OES/MS; pXRF
PAL5	16	5B	G	4	microCT; OM; XRD; ICP-OES/MS; pXRF
PAL6	18	1	A	4,3	microCT; OM; XRD; ICP-OES/MS; pXRF
PAL7	13	1	C	2,1	microCT; OM; XRD; ICP-OES/MS; pXRF
PAL8	3	3	C	-	microCT; XRD; pXRF
PAL9	7	4	L	4,6	microCT; OM; XRD; ICP-OES/MS; pXRF
PAL10	4	5B	E	-	microCT; pXRF
PAL11	19	5 A	L	5,3	microCT; OM; XRD; ICP-OES/MS; pXRF
PAL12	8	4	L	-	microCT; OM; pXRF
PAL13	9	4	V	-	microCT; XRD; pXRF
PAL14	10	4	L	-	microCT; pXRF
PAL15	6	5B	Q	-	microCT; pXRF
PAL16	14	1	L	-	microCT; pXRF
PAL17	5	5B	E	5,6	microCT; OM; XRD; ICP-OES/MS; pXRF
PAL18	17	5B	A	5,3	microCT; OM; XRD; ICP-OES/MS; pXRF

targeted materials from phases 5 and 4, with some attention given to phases 3 and 1. This decision stemmed from the necessity to comprehend a little-known transitional period between the SMP culture and the Late Neolithic, predominantly documented at Palù di Livenza during phases 4 and 5 (for further details, refer to Visentini 2018). Regarding the early phases (1–4), particular attention was placed on four-spouted vessels (PAL 9, 12, 13, 14), which are representative elements of the period (Figs.S2, S4). For the Late Neolithic (phase 5; Fig. S1), characterized by a significant number of pottery finds, focus was placed on the most distinctive and prevalent types, including vases, bowls, and coarse paste ollae adorned with impressed decorations (PAL 2) or plastic ornaments like impressed cords (PAL 5), as well as ashlars and tablets featuring central depressions (PAL 1). This phase is associated with finer pottery finds and one vessel of this group has been analysed too (PAL 10).

Regarding phase 3, only one artefact underwent analysis (PAL8). Its typological characteristics, such as channeled decoration and a burnished surface, appear to be reminiscent of the Eastern Adriatic area, specifically the Late Hvar style (Fig. S3). This association is primarily due to the polished surface treatment and the presence of vertical ribs on the sides of the handle (for comparisons, refer to Forenbaher et al. 2013; Fig. 3.8; Marijanović 2005; T. XXXVI).

Concerning the chronologically older phase 1, a particular point of interest is the artefact featuring a series of deep impressions and a subcutaneous handle (PAL 16; Fig. S4). This artefact can be attributed to an early phase of the third style of the SMP culture. This attribution is supported by comparisons with artefacts from other sites in north-east Italy, such as Bannia-Palazzine di Sopra (province of Pordenone), Meolo (province of Venezia), Bernardine di Coriano (province of Verona), and Gazzo Veronese-Scolo Gelmina (province of Verona) (Visentini 2018).

A few additional shards belonging to macroscopic groups A and E were also analysed (PAL 17 and PAL 18). In both cases, the samples displayed some distinctive attributes and were considered as variants of their respective paste type useful for testing the validity of the macroscopic selection criteria through the archaeometric analysis.

Methods

All artefacts were analysed by means of microCT, which allows, in a non-destructive manner, to obtain microstructural morphological information useful for reconstructing the pottery forming technology of the vases and obtaining a morphologic description of the pastes. Mineralogical (X-ray diffraction - XRD), petrographic (optical microscopy - OM) and chemical (Inductively Coupled Plasma Optical Emission and Mass Spectrometry – ICP-OES and ICP-MS) analyses were conducted on ten selected vessels from which it was possible to detach small samples (Table 1) in order to achieve a complete characterisation of the ceramic bodies. At the same time, a non-destructive portable X-ray fluorescence (pXRF) analysis has been carried out on all the samples and its quality has been tested on the basis of ICP-OES/MS results. Finally, the pXRF data have been statistically evaluated through principal component analysis (PCA).

X-ray computed microtomography (microCT)

The samples were analysed at the Multidisciplinary Laboratory of the Abdus Salam International Centre for Theoretical Physics (ICTP) in Trieste, using a system designed for the study of archaeological and paleoanthropological materials (Tuniz et al. 2013), which has already been successfully applied to study ancient pottery (Bernardini et al. 2013, 2015, 2016, 2019; Caloi and Bernardini 2024). The ICTP's microCT system was specifically designed for the analysis of large objects (about 20 cm for a weight of up to 15 kg), with a voxel size of about 30–50 μm (smaller volumes are usually analysed with a voxel size of about 10–20 μm). The sample holder and the source-detector system are mounted on a flexible mechanical set-up that allows the components to be moved according to the characteristics of the samples and the resolution desired.

The microCT scans were carried out by using a sealed X-ray source (Hamamatsu L8121-03) with a focal spot size of 5 μm and a flat panel detector (Hamamatsu C7942SK-25; pixel size of 50 μm) according to the following parameters: 110 kV, 90 μA, exposure time/projection of 2 s, 1800 projections of the samples over 360°. The X-ray beam was filtered by a 0.1 mm-thick copper absorber. The final slices were reconstructed using the commercial software DigiXCT (Digisens) in 32-bit format, at an isotropic voxel size from 24 to 39 micron.

Preliminary information on the primary production technology was deduced mainly from the three-dimensional models obtained by microCT. By producing virtual sections of the vessel walls, it is possible to identify macrostructural features, such as voids and joins, that often allow the primary forming techniques used to be identified (Kahl and Ramminger 2012; Bernardini et al. 2013, 2015, 2016, 2019; Sanger 2016; Machado et al. 2017; Thér 2020). In our study we have decided not to apply time-consuming 3D analysis and quantification of particle and voids orientation, even if this relatively innovative approach has recently provided encouraging, but still preliminary, results for the analysis of small volumes of experimentally produced vessels (e.g. Gait et al. 2022). The observation of technological joins in the virtual volumes of the investigated vessels has allowed to identify in most of them clear discontinuities produced by the primary forming processes. In order to verify the presence and orientation of technological joins, we have produced a large number of virtual sections perpendicular to the wall surface along the vertical direction. At the same time, we have observed the areas of interest through horizontal and tangential virtual sections too (for the orientation of the sections see Rye 1981, 67–87; Woods 1985).

Optical microscopy (OM)

Thin sections were produced from the fragments detached from the finds at the LAMA-Laboratory for Analysing Materials of Ancient origin of the Iuav University of Venice. The thin sections allowed the samples to be observed and studied in transmitted light with a Leitz-Wetzlar binocular polarising microscope at the Department of Mathematics, Informatics and Geosciences of the University of Trieste. The fabric of the analysed vessels has been described following the indications given by Whitbread (2016).

X-ray powder diffraction (XRD)

X-ray diffraction patterns of 12 samples were obtained on powdered samples spread out on aluminium plates using a STOE D 500 X-ray diffractometer at room temperature at the Department of Mathematics and Geosciences of the Trieste University. CuKα radiation was used through a flat graphite crystal monochromator. The current and the voltage were set at 20 mA and 40 kV, respectively. The scanning angle ranged from 2 to 60° of 2θ, steps were of 0.1° of 2θ, and the counting time was of 2 s/step. Mineral phases have been recognized by using Hanawalt Manual (JCPDS 1993).

Inductively coupled plasma Optical Emission and Mass Spectrometry (ICP-OES and ICP-MS)

The samples were powdered using an agate mill at a 150-mesh fraction in the laboratory of Department of Mathematics, Informatics and Geosciences of Trieste University. Major and trace element determinations of 10 vessels (Table 1) were carried out by ICP-OES and ICP-MS, respectively, at the Centre de Recherches Pétrographiques et Géochimiques (CNRS) Vandoeuvre, France. The analytical uncertainties are estimated at between 5 and 10% (Govindaraju and Mevelle 1987).

Portable X-ray fluorescence (pXRF)

Non-destructive elemental analyses of original samples, via directly analysing the sample surfaces, were performed via pXRF: an Olympus Vanta C Series with a 4 W Ag anode X-ray tube (VCA) with silicon drift detector. The VCA has an excitation source ranging from 8 to 50 keV and can detect elements from magnesium (Mg) to uranium (U). As is the case with many pXRF instruments, there are various factory methods available, each with different calibrations. The "Soil" method is more suited for trace concentrations, whereas the "Geochem" method is more accurate at higher concentrations. To determine as many elements as possible with the best data quality both methods were used (Ross et

al. 2014) without moving the analyser between two measurements (Lemière 2018). In this study, pXRF data > 1 wt% were selected from the geochem method, whereas values < 1 wt% were determined using the soil method. Both methods used three beams set to 30 s each, with a total of 1.5 min for single analysis. The total number of analyses for each sample was 4, consisting in 2 replicates for 2 different spots of the sample surface. The accuracy was evaluated by means of certified reference materials (CRMs; "PACS-3" and "MESS-4", Marine Sediment, NRCC, Whitehorse, YT, Canada), which were analysed in the same batch of samples using both methods.

Validation of pXRF data

Data processing for statistical analysis was conducted with Python (e.g., SciPy packages). For further statistical analysis and data quality levels for pXRF results, the US EPA (1998) procedure was followed according to the majority of recent studies, e.g., (Al-Musawi and Kaczmarek 2020; Barago et al. 2022; Rouillon and Taylor 2016; Shuttleworth et al. 2014). For this study, pXRF data of original samples (10 out of 18 samples) were compared to ICP-OES/MS data of the same samples (powders), to evaluate if pXRF is suitable for quantitative chemical measurements of heterogeneous and unground samples, allowing to analyse all 18 samples. Comparability of pXRF with confirmatory data (ICP-OES/MS) was assessed using linear regression statistics, where optimal correlations were found with a coefficient of determination $r^2 = 1$, slope equal to 1, and intercept with the x- and y-axis equal to 0. To ensure that both high and low values had equal influence on the correlation, all data were $\log_{10}$ transformed. Values below limit of quantification (LOQ) were not considered for data validation. Z-test was used to test the statistical similarity between (1) the slope of the linear regression curve and an ideal slope = 1 and (2) between the y-intercept of the regression function and an ideal y-intercept = 0. A t-test was also performed on $\log_{10}$-transformed data to determine if the pXRF and the ICP-OES/MS data, for each element, belonged to the same population. This would imply that there are no significant differences between the two analytical techniques occurred. The t-Test, slope and y-intercept z-tests are considered successful for p-value > 0.05. Lower values of p-value imply significant differences between sample populations or from the ideal slope and y-intercept and vice versa. According to criteria established by the US EPA (1998), 3 levels of quality of pXRF can be defined. (1) The definitive level is considered to be the highest quality level. (2) Quantitative screening level data provides the quantification, though it may be relatively imprecise. (3) Qualitative screening level data indicates the presence or absence of elements of interest but does not provide reliable concentration estimates (Table 2).

Repeatability (or precision), was determined on replicates for each analyte and technique by RSD% as:

$$(Standard\ deviation\ /\ mean)\ X\ 100$$

Data statistical analysis

Biplot associated with principal component analysis (PCA) was calculated on log10 transformed pXRF data for the elements with "quantitative" or "definitive" data quality level. For PCA analysis, values below LOQ were considered as LOQ / 2. Calculation was performed in Python via the Scikit-learn library (Pedregosa et al. 2011). Biplot is an explorative graph where samples are displayed as points while variables (elements) as vectors. Test were successfully performed to determine if data suited for factory analysis: Barlett's sphericity test resulted successfully with $p < 0.001$ and KMO = 0.73 (Kaiser-Meyer-Olkin test; acceptable values for KMO > 0.5).

Results

MicroCT

Among the hand-building forming techniques without rotational kinetic energy (RKE according to the definition of Roux 2017, 2019), the most common are the coil- and slab-building, pinching, moulding and beating (Thér 2020). Most of them are characterised by simple compressive deformation perpendicular to the vessel wall with the only exception of the coiling technique. Coil-building is generally based on a roll of clay wrapped in a spiral, with one hand inside the vessel and one outside as support. The forming of the coils is characterised by compression with a revolving movement

Table 2 US EPA criteria for establishing data quality

Data Quality Level	Statistical Parameter
Definitive	$r^2 = 0.85$ to 1.0. The repeatability (RSD%) must be less than or equal to 10%, and inferential statistics indicate the two data sets are statistically similar.
Quantitative screening	$r^2 = 0.70$ to 1.0. The RSD% must be less than 20%, but the inferential statistics indicate that the data sets are statistically different.
Qualitative screening	r^2 = less than 0.70. The RSD% is greater than 20%. The data must have less than a 10% false-negative rate.

of the deformed mass while the assembling of the coils is carried out through compression and shear deformation. Due to such peculiar forming process, orientation of voids and particles in the coil-built vessels is different compared to that one of pottery produced by compressive techniques, such as pinching, slab-building, moulding and beating, all characterised by a similar orientation pattern.

In vertical and tangential sections of coil-built vessels the voids and particles are non-aligned and horizontally aligned, respectively. In vertical and tangential sections of vessels produced using compressive techniques, voids and particles are generally parallel to the wall surface in the vertical slices, while they are weakly oriented or non-oriented in the tangential sections (Berg 2008; Thér 2020).

Considering macro-structural joins, coil-building is identifiable in either real or virtual vertical sections of vessel walls through transversal discontinuities extending from one face of the vessel to the other (see, for instance, Lindahl and Pikirayi 2010; Bernardini et al. 2019). Lindahl and Pikirayi (2010; fig. 8) have categorized two coiling techniques based on the orientation of these discontinuities: the U-technique and the N-technique (Lindahl and Pikirayi 2010; fig. 6). The former is distinguished by a noticeable curvature of the pores/joins with the bottom oriented upwards, whereas the pores/joins formed by the N-technique display a diagonal orientation.

The macro-structural joins identified in the majority of the vessels (PAL1-2, PAL4, PAL6; Fig. S1: PAL1-2, PAL4-7, PAL9, PAL10, PAL12, PAL14; Table 3; Fig. 2a) indicate that most of them were produced by the N-coiling technique. This finding is especially interesting in relation to the four-spouted pots, as it confirms the hypothesis based on macroscopic observation. The production of the four-spouted vessels likely employs the same technology as the round-mouthed ones and may even represent a variation of the same vessel type.

Only the vessel PAL15 could have been produced by a compressive technique, perhaps pinching, considering the very small size of the vessel, and the external part of the base seems to have been refined adding some layers of clay (Fig. 2b).

Considering the paste composition, the main lithic inclusions can be divided into two main groups: homogeneous-density and variable-density rock fragments (Table 3; Fig. 3). Given their size (up to about 10 mm) and angular morphology (see Fig. 3), it is probable that these large fragments mostly correspond to crushed rock fragments added to the paste as temper material.

Table 3 Summary of microCT analysis results. The colours used to highlight the samples represent the identified chronological phases: grey: phase 1; yellow: phase 3; green: phase 4; blue: phase 5; xxx, abundant; xx, frequent; x, rare

Sample	Grain-size	Homogenous-density inclusions	Variable-density inclusions	Voids likely from carbonate inclusions	Low-density inclusions	Technology
PAL1	coarse	x	xxx	-	-	coiling
PAL2	coarse	xxx	x	-	x	coiling
PAL3	medium	xxx	-	-	-	-
PAL4	coarse	xx	x	-	-	coiling
PAL5	coarse	xx	x	-	-	coiling
PAL6	coarse	-	x (only in the handle)	xxx (in the wall of the vessel)	-	coiling
PAL7	coarse	xxx	-	-	-	coiling
PAL8	fine	-	x	-	-	-
PAL9	coarse	-	-	xxx	x	coiling
PAL10	fine	xx	xxx	-	-	coiling
PAL11	medium	-	-	xx	x	-
PAL12	medium	x	-	x	x	coiling
PAL13	coarse	x	xxx	-	-	-
PAL14	medium/coarse	-	-	xx	x	coiling
PAL15	medium	-	-	xx	-	pinching ?
PAL16	coarse	xxx	-	x (small voids)	-	-
PAL17	fine	x	-	-	-	-
PAL18	coarse	x	-	xxx	-	-

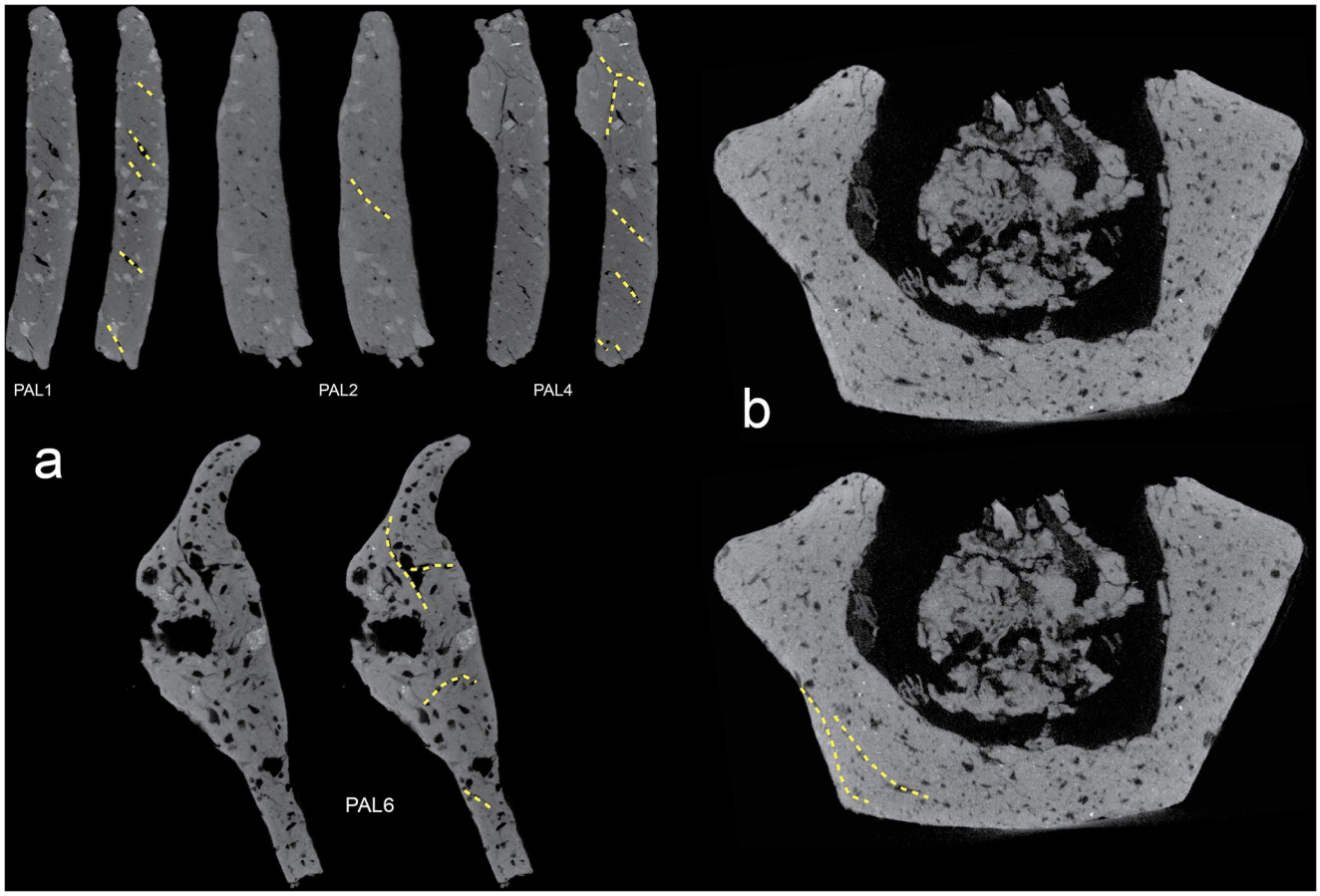

Fig. 2 (**a**): Vertical virtual sections of the rims of selected artefacts showing main technological macro-structural joins, highlighted by dashed yellow lines. (**b**): Vertical virtual section of the small vessel PAL15 where the typical discontinuities related to the coiling technique are not visible. At the same time, two external layers of clay, shown by the dashed yellow lines, were used to refine the bottom of the vessel. Images not to scale

Several samples show abundant and large voids (Fig. 3, mainly PAL6, PAL9, PAL14, PAL18). The virtual extraction of such voids from PAL18 (Fig. 4) distinctly reveals that the original lithic inclusions consisted of large angular lithic fragments, with smoothed edges, reaching sizes of about 10 mm. In their review on the presence of calcite in archaeological pottery, Fabbri et al. (2014) emphasize the possibility of calcite residues, termed "calcite ghosts," arising from dissolution processes. Such processes can occur when pottery is exposed to acidic water solutions during burial in soil.

In the case of sample PAL6, a paste with variable-density inclusions and voids possibly derived from the original carbonate temper was used to shape the handle, while the walls of the vessel are characterised by variable-density rock fragments (Fig. 2a), demonstrating that different paste recipes were used at site at the same time. This observation is especially significant as it supplements the macroscopic analysis of the entire pottery complex. It was noted that in the majority of cases, plastic decorations such as handles, tubercles, ashlars, and cords were separately applied to the surface of the vessels using pins.

X-ray diffraction

From a mineralogical point of view, XRD analysis has revealed that all 12 analysed samples are similar and composed mainly of quartz; subordinate plagioclase has been detected in some of the samples. It is worth noting that clay minerals/phyllosilicates, possibly illite and/or montmorillonite, are present in trace amounts in about 80% of the samples (Fig. 5; for all diffractograms see supplementary material S2).

Optical Microscopy

The samples generally show quite similar petrographic features (Table 4). They are characterized by a dark-brownish clay matrix mainly containing quartz, muscovite and chert. Often, the samples host large rock fragments (from 0.5 to

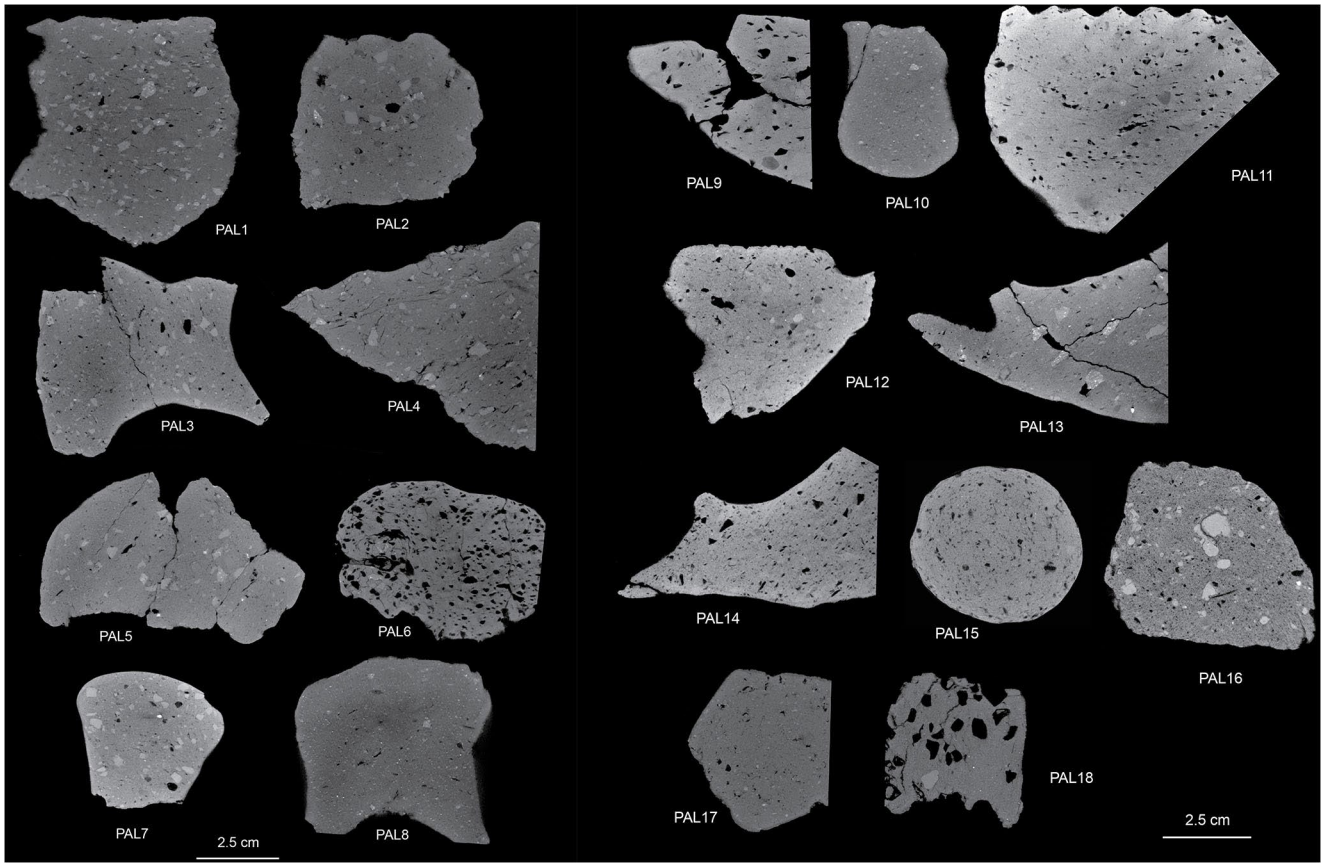

Fig. 3 Virtual sections of the analysed findings obtained by microCT

4 mm), which generally show a metamorphic origin, rarely magmatic and sedimentary characteristics. The metamorphic rock fragments consist either of purely polycrystalline quartz or polycrystalline quartz with muscovite, lacking apparent foliation (both labelled quartzite, see below).

Three fabric groups have been recognised based on the presence of large (from about 0.5 to 10 mm) sub-angular to sub-rounded voids (Fabric 1), large (from about 0.5 to 4 mm) rock fragments (Fabric 2) or both (Fabric 3).

Fabric 1 (samples PAL6, PAL9 and PAL11) shows a homogeneous and brownish clay matrix containing numerous large voids (from about 0.5 to 10 mm) and micro-inclusions without apparent preferential orientation. Inclusions range from 0.01 to 0.4 mm. The grain size distribution is poorly sorted and varies unevenly in size. Inclusions are mostly sub-angular to sub-rounded, with occasional angular and rounded grains (Fig. 6c).

Abundant inclusions: quartzite (0.2 to 0.4 mm), generally well rounded to sub-rounded, rarely sub-angular, composed by well sorted quartz with undulose extinction and rarely small-sized muscovite and without clear foliation; monocrystalline quartz (0.05–0.1 mm), poorly sorted, from angular to sub-rounded and rarely rounded with undulose to direct extinction (Fig. 6c-d). Abundant to rare inclusions: well sorted muscovite (0.01 to 0.05 mm); chert (0.01 to 0.3 mm), moderately sorted, sub-angular to sub-rounded (Fig. 6d). Rare inclusions: well sorted biotite (0.01 to 0.05 mm).

Rare grog grains (type 1) range from 0.2 to 0.5 mm in size. They are angular to sub-angular, prolate to equant in shape and exhibit similar characteristics to the pottery (for the grog properties see Whitbread 1986), such as a dark-brown colour and contain quartz, chert, and muscovite.

Large voids characterise Fabric 1. They range from 0.5 to 3.0 mm in thin sections (Fig. 6g-h), up to 10 mm in microCT virtual slices (Figs. 3 and 4), and likely result from carbonate lithic fragments (see below). They exhibit shapes varying from sub-angular to sub-rounded, typically without any preferential orientation.

Fabric 2 (samples PAL1, PAL3, PAL4, PAL5, PAL7 and PAL17) shows a homogeneous and brownish clay matrix containing large to micro-inclusions without apparent preferential orientation, ranging from 0.01 to 4.0 mm. The grain size distribution is poorly sorted and varies unevenly in size. The majority of inclusions are sub-angular to sub-rounded, with occasional angular and rounded grains (Fig. 6a-b).

Abundant inclusions: quartzite (0.2 to 4.0 mm), generally sub-rounded to sub-angular, without clear foliation

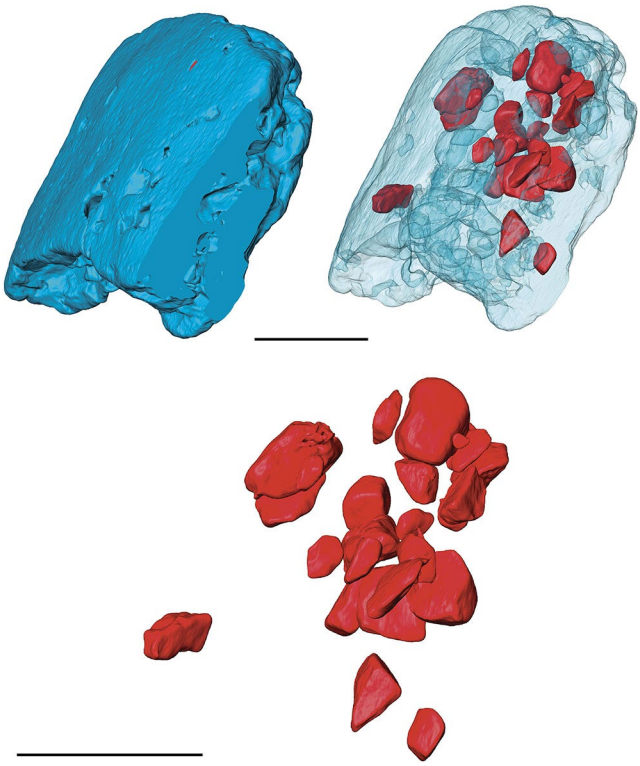

Fig. 4 Virtual extraction of voids, most likely corresponding to original carbonate lithic temper material, from PAL18. Scale bars: 1.5 cm

and composed by well sorted quartz with undulose extinction and rarely containing small-sized muscovite (Fig. 6b); monocrystalline quartz (0.05–0.5 mm), poorly sorted, from angular to sub-rounded and rarely rounded with undulose to direct extinction. Abundant to rare inclusions: well sorted muscovite (0.01 to 0.05 mm); chert (0.01 to 0.05 mm), moderately sorted, sub-angular to sub-rounded (Fig. 6a). Rare inclusions: well sorted and often altered biotite (0.01 to 0.05 mm); terrigenous rock fragments, mostly pelite (about 0.5 mm), well rounded and composed of very fine and well sorted silica-carbonate grains; a single igneous rock fragment (trachyte?; 0.5 mm), sub-rounded composed by quartz that shows a normal extinction, feldspar and partially altered biotite (Fig. 6a).

Abundant to rare grog grains (type 1) range from 0.2 to 1.0 mm (Fig. 6e-f). They are angular to sub-angular and prolate to equant in shape (for the grog properties see Whitbread 1986), showing similar features than the pottery (i.e. dark-brown colour with quartz, chert and muscovite). In Pal17 a grog hosts a carbonate clast of 0.2 mm (Fig. 6f). A different type of probable grog (type 2; 0.3–0.8 mm) has been identified too (Fig. 6e). It is sub-angular, showing a yellow-brownish groundmass colour and composed by smaller minerals clasts that are hardly recognizable.

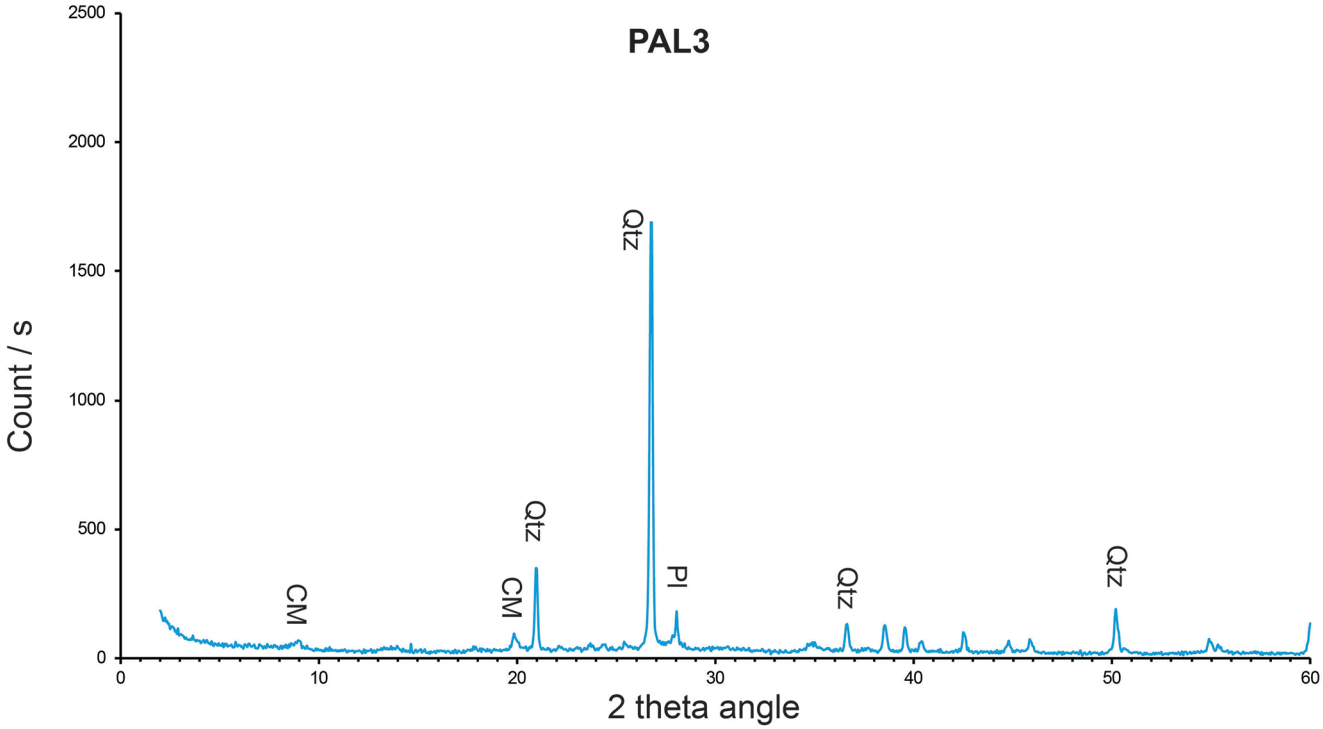

Fig. 5 Selected representative XRD spectrum. CM: clay minerals; Qtz, quartz; Pl: plagioclase.

Table 4 Petrographic features of the vessels analysed by optical microscopy. Samp, Sample; Rock frag, Rock fragment; Mu, Muscovite; xxx, abundant; xx, frequent; x, rare

Samp	Grainsize	Large (≥ 0.5 mm) rock frag	Rock frag type (all grain sizes)	Carbonate ghost	Grog	Quartz	Mu	Chert	Biotite
Pal1 (fabric 2)	medium-fine	xxx	quartzite and igneous		x	xxx (from angular to rounded)	xxx	xx	
Pal3 (fabric 2)	medium-coarse	xxx	quartzite			xxx (from angular to sub-rounded)	x	xx	
Pal4 (fabric 2)	fine	xxx	quartzite			xxx (angular)	xxx	x	
Pal 5 (fabric 2)	coarse	xxx	quartzite			xxx (angular)	x	xx	
Pal 6 (fabric 1)	fine		quartzite	xxx	x	xxx (from angular to sub-rounded)	xx		
Pal 7 (fabric 2)	medium-fine	xxx	quartzite and terrigenous		x	xxx (from angular to rounded)	xxx	x	x
Pal 9 (fabric 1)	medium-coarse		quartzite	xxx	x	xxx (from angular to sub-rounded)	xxx	x	
Pal 11 (fabric 1)	coarse		quartzite	xx		xxx (from angular to sub-rounded)	x	xxx	x
Pal 12 (fabric 3)	medium-coarse	x	quartzite and terrigenous	xx		xxx (from angular to sub-rounded)	xxx	x	
Pal 17 (fabric 2)	medium-fine	x	quartzite		xxx	xxx (from angular to rounded)	x	x	
Pal 18 (fabric 3)	coarse	x	quartzite	xxx		xxx (from angular to sub-rounded)	xxx	xx	

Fabric 3 (samples PAL12 and PAL18) shows a homogeneous and dark brownish (PAL12) or brown yellowish (PAL18) clay matrix containing several large voids and large to micro-inclusions without apparent preferential orientation, ranging from about 0.01 to 4.0 mm. The grain-size distribution is poorly sorted and uneven in size. Inclusions are mainly sub-angular to sub-rounded with rare angular and rounded grains.

Abundant inclusions: quartzite (0.2 to 4.0 mm), generally well rounded to sub-rounded, rarely sub-angular, composed by well sorted quartz with undulose extinction and rarely small-sized muscovite and without clear foliation; monocrystalline quartz (0.05–0.1 mm), poorly sorted, from angular to sub-rounded and rarely rounded with undulose to direct extinction; well sorted muscovite (0.01 to 0.05 mm). Frequent to rare inclusions: terrigenous rock fragments, mostly pelite (about 0.5 mm), well rounded and composed of very fine and well sorted silica-carbonate grains; chert (0.01 to 0.03 mm), moderately sorted, sub-angular to sub-rounded.

Large voids, ranging from 0.5 to 3.0 mm in thin sections, up to 10 mm in microCT virtual slices, are present in Fabric 3 too. They likely result from carbonate lithic fragments. They exhibit shapes varying from sub-angular to sub-rounded, typically without any preferential orientation.

Interestingly enough, carbonate rock fragments have not been identified with the exception of a few fragments included within a grog in sample PAL17 (Fig. 6f). As already reported above, it is likely that carbonate rock fragments, originally included in some of the vessels, have been dissolved by weathering processes in the soil leaving the empty voids that are clearly visible in the microCT virtual renderings of several samples (Table 3; Fig. 4; Fabbri et al. 2014) and in thin sections. The few identified carbonate inclusions, mentioned above, may have been preserved from chemical dissolution because they were contained within a grog grain.

This interpretation is supported by the lack of reaction rims (Fig. 6g-h), typically formed at high temperatures as a result of the interaction between the coarse carbonate inclusions and the surrounding fired clay (Fabbri et al. 2014).

According to the size, up to about 4 mm in thin section and 10 mm in microCT virtual slices (Fig. 3), and the sub-angular or angular morphology of the large lithic inclusions in Fabric 2 and 3, it is possible that most of them were added to the paste as tempering material. Their rock types (i.e. prevalent quartzite and few igneous and terrigenous sedimentary clasts) could be indicative of a region of polygenic sedimentary rocks containing metamorphic, magmatic and carbonate clasts.

The large voids in Fabric 1 and 3 likely result from large carbonate clasts. Such carbonate fragments were likely added to the paste as tempering material obtained crushing limestone.

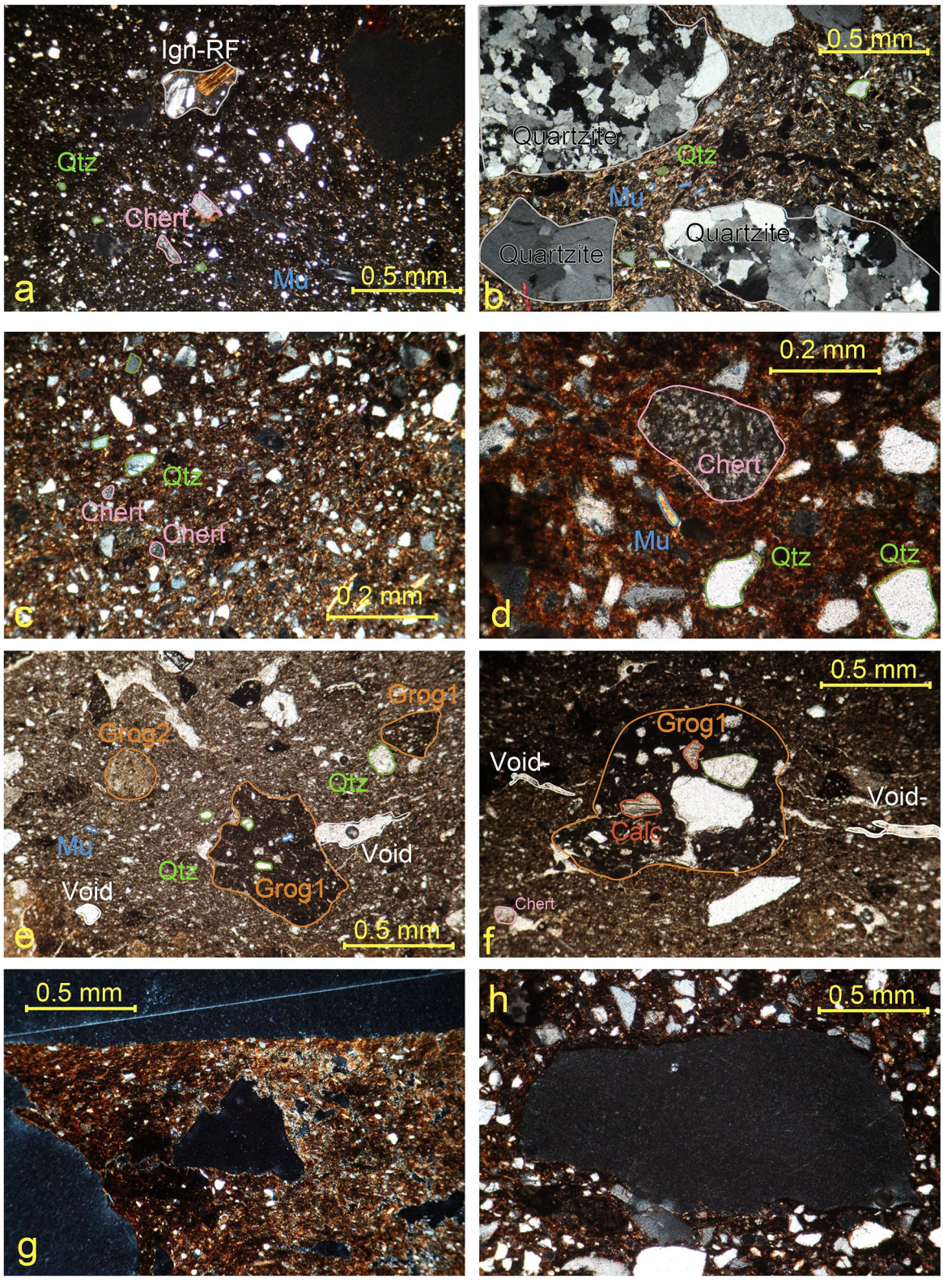

Fig. 6 Microphotographs of selected thin sections: a = PAL1; b = PAL7; c = PAL9; d = PAL11; e-f = PAL17; g = PAL6; h = PAL11. Photographs a-d and g-h taken using crossed polars; photographs e-f taken using plane-polarised light. Mu, muscovite; Qtz, quartz; Ign-RF, igneous rock fragments; Calc, calcite or dolomite

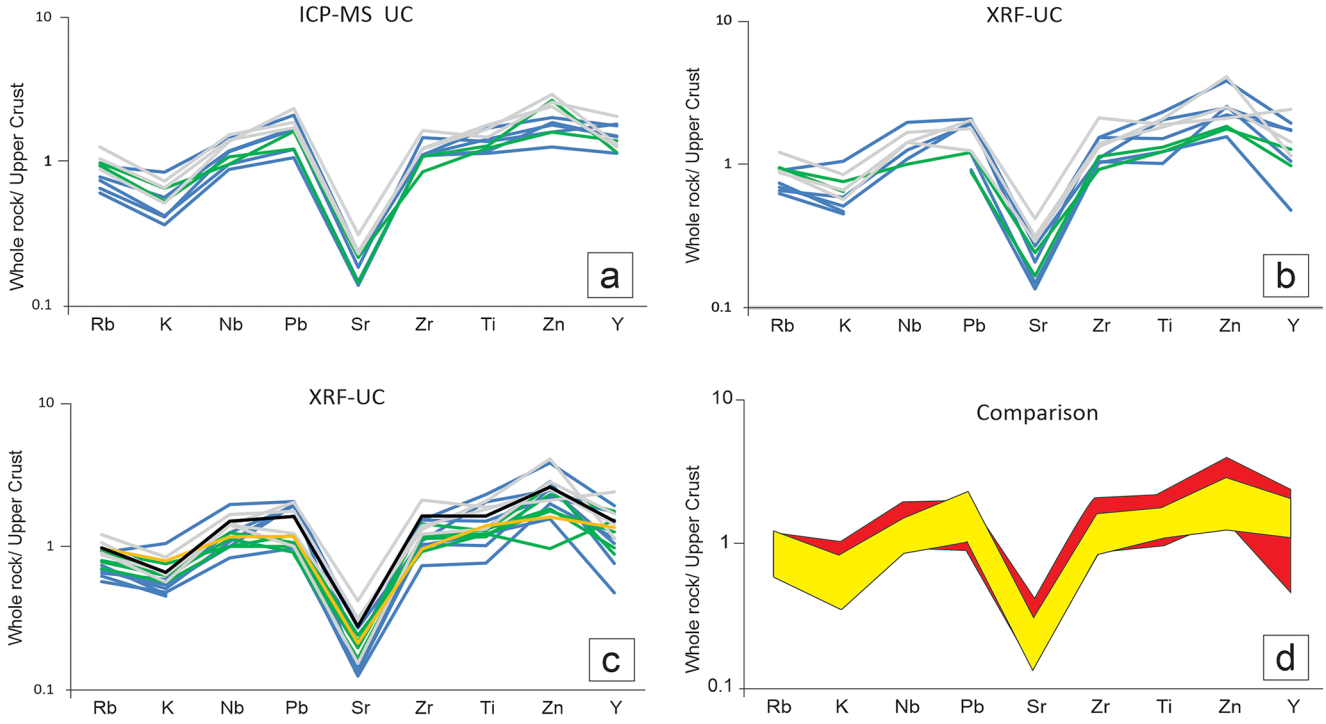

Fig. 7 Upper crust normalised (Rudncik and Gao 2004) spider diagrams of the samples analysed by both ICP-OES/MS (**a**) and pXRF (**b**), all samples analysed by pXRF (**c**) and a comparison between ICP-OES/MS and pXRF data fields (**d**); yellow field: ICP-OES/MS; red field: pXRF). Grey patterns: phase 1; yellow pattern: phase 3; green patterns: phase 4; blue patterns: phase 5

Table 5 Statistical summary of comparability between pXRF and ICP-OES/MS log10 transformed chemical data. More exhaustive statistical information is provided in Table S2. RSD: relative standard deviation, indicator of replicability. r2 and slope derive from the linear regression analysis. A Data quality levels are defined by US EPA (1998); b relative standard deviation; * significant for $p < 0.05$

Element	Data quality[a]	*n* data	RSD[b]	r^2	Slope
K	Quantitative	10	1%	0.82*	0.89
Ti	Quantitative	10	1%	0.80*	1.54
Nb	Quantitative	7	10%	0.78*	1.26
Pb	Quantitative	10	8%	0.74*	1.14
Rb	Definitive	10	1%	0.89*	0.86
Sr	Quantitative	10	5%	0.98*	1.35
V	Quantitative	10	5%	0.84*	0.60
Y	Quantitative	9	14%	0.77*	1.40
Zr	Quantitative	10	3%	0.77*	1.21

Chemical results

ICP-OES/MS

The chemical composition of the samples, obtained by ICP-OES/MS (Table S1; Fig. 7a) and normalized to the upper crust (Rudnick and Gao 2004), exhibits a slight negative anomaly in K and positive anomalies in Pb and Zn. Sr shows a notably pronounced negative anomaly, likely linked to the absence of carbonate material in the sample, as confirmed by the low Ca content (Table S1). The other elements align closely with crustal values.

Notably, in Fig. 7a samples from phase 4 are positioned below samples from phase 1 for all elements while maintaining an identical pattern. In this case, a dilution effect is hypothesized due to the higher presence of quartz in samples from phase 4 compared to phase 1 (Table S1).

In comparison, samples from phase 5 cover the entire field represented by the other groups, showing variable Si contents (Table S1).

Validation of pXRF data

The validation process, comparing the pXRF data with the ICP-OES/ICP-MS data, has demonstrated a good level of reliability for the elements listed in Table 5. The compositional variations between the two methods are also reported in Fig. 8. Figure 7a-b shows the spider diagrams of the elements analysed by ICP-OES/MS and pXRF, which have been validated as more reliable. The two diagrams display similar anomalies and trends, making them very well comparable.

pXRF data and PCA

Having confirmed the reliability of the values obtained through pXRF (Table S2) for the elements listed in Table 5; Fig. 7c presents the spider diagrams of all the specimens analysed using pXRF, including those that were not studied through destructive ICP-OES/MS. The diagrams exhibit similar patterns, indicating a general chemical homogeneity

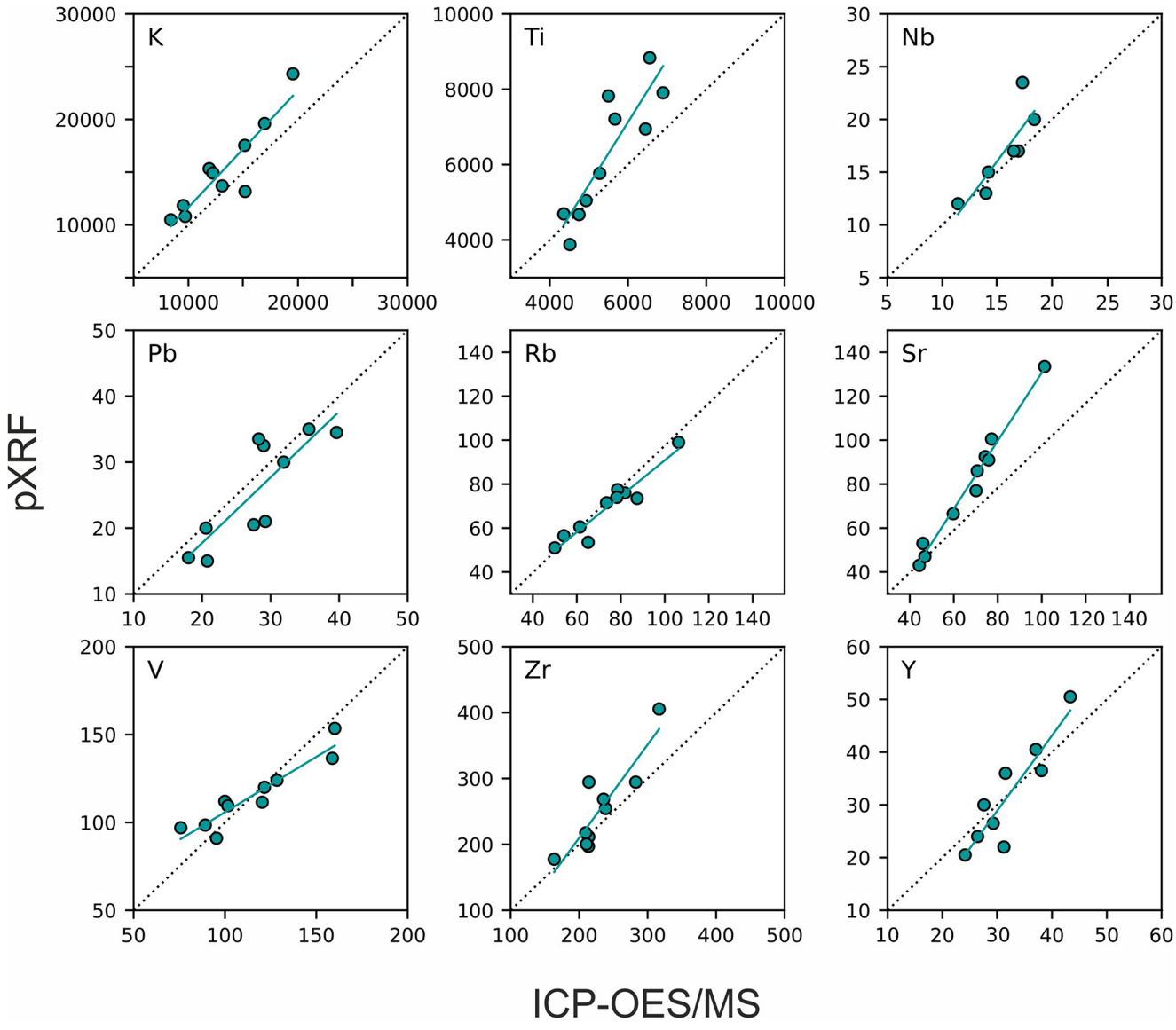

Fig. 8 Comparison of analysed concentrations of major and trace elements between pXRF and (confirmatory) ICP-OES/MS chemical data

within the investigated material assemblage, and do not allow to differentiate the three fabrics identified through optical microscopy. The PCA analysis of the most reliable pXRF data confirms the overall similarity among the samples. However, it also indicates the presence of sub-groups with very similar chemical characteristics, which can be partially associated with their different chronologies and typologies (Fig. 9). Several samples belonging to phase 5, but in particular samples PAL2, PAL5 and PAL11 (all vessels showing a rim with finger impressions) plot quite close in the left part of the biplot (Fig. 9, blue symbols). The samples belonging to phase 4 PAL13 and PAL14 share an almost identical chemical composition and the other samples with the same chronology fall quite close too (Fig. 9, green symbols). The vessels of phase 1 are mostly located in the right part of the biplot (Fig. 9, grey symbols). Such similarities suggest that slightly different local raw material sources were exploited and/or specific recipes were in use through time. It is important to mention that the samples located in the left quadrants of Fig. 9, which are characterized by lower concentrations of the elements used as variables for the PCA, show a notably high abundance of quartz grains. Therefore, the observed lower concentration of the elements being studied is likely a result of a dilution effect caused by the higher quartz content, which naturally contains very small amount of such elements. Such dilution effect was already detected observing the spider diagrams of Fig. 7a and is confirmed by the Si content measured by ICP-OES/MS. For example, the SiO_2 (wt%) contents in vessels PAL5 and PAL11, located in the leftmost part of the diagram, are much higher (i.e., 73.31

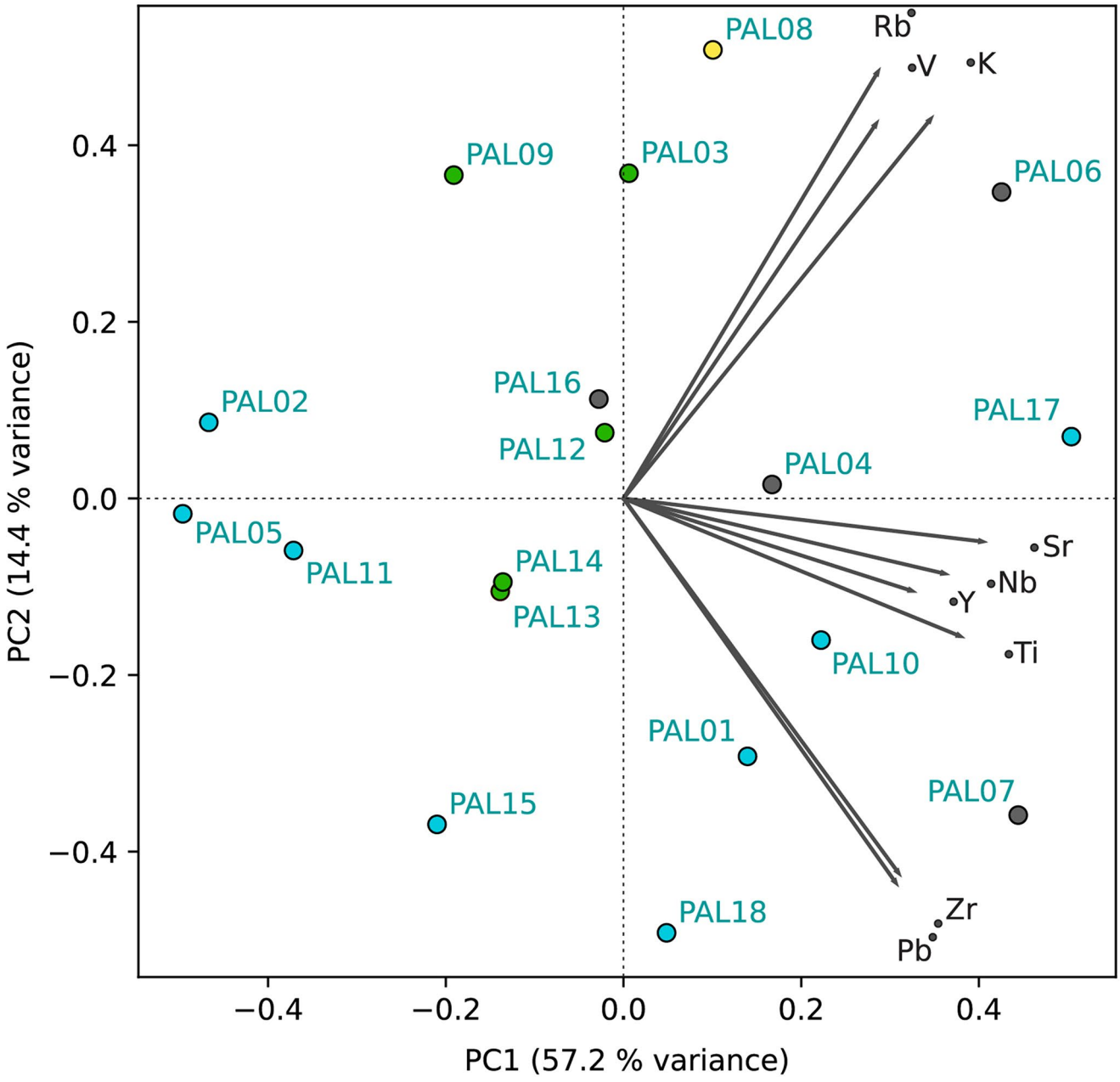

Fig. 9 Biplot of samples and variables (elements) calculated with validated pXRF data for all samples. Grey samples: phase 1; yellow sample: phase 3; green samples: phase 4; blue samples: phase 5

and 69.31, respectively) than the SiO_2 value in samples located in the rightmost part of the diagram, such as PAL6 and PAL17 (i.e., 52.12 and 46.10, respectively).

Discussion and conclusions

N-coiling technique seems to have been the main primary forming technique for the analysed pottery sherds, including the four-spouted vessels, given visible evidence in microCT virtual sections.

Three main fabrics, not well comparable with macroscopic groups, have been distinguished in thin sections primarily through the presence of different lithic inclusions. The first group (Fabric 1) includes vessels characterised by sub-angular to sub-rounded voids (ranging from about 0.5 to 10 mm) interpreted as carbonate ghosts (samples PAL6, PAL9 and PAL11; Fabbri et al. 2014). The second group (Fabric 2) consists of vessels containing large (ranging from about 0.5 to 4 mm) rock fragments (samples PAL1, PAL3, PAL4, PAL5, PAL7 and PAL17). The third group (Fabric 3) encompasses vessels containing both large rock fragments

and calcite ghosts (samples PAL12 and PAL18). According to microCT virtual slices (Fig. 3), samples PAL14-15 should belong to Fabric 1, while PAL2 and PAL13 to Fabric 2. It is possible that the rock fragments, categorized as homogeneous-density and variable-density in microCT data, mainly consist of quartzite.

The size and the angular morphology of the large lithic inclusions in Fabric 2 and 3, especially evident in microCT virtual slices (see especially PAL1-5, PAL7 and PAL13 of Fig. 3), suggest they were added to the paste as tempering material. The same applies to the calcite ghost, suggesting that crushed carbonate was originally used to temper Fabric 1 and 3. Crushed ceramic tempering is documented in in fabrics 1 and 2.

There is no correlation between the three fabric groups identified and the chronological phases determined from stratigraphic evidence. It appears that these fabrics were in use throughout the entire duration of the settlement.

The absence of preserved carbonate inclusions, confirmed by OM, XRD, and chemical analyses, alongside the presence of angular voids, up to about 10 mm in size as observed in multiple samples and clearly visible in the microCT datasets (Fig. 3), have been attributed to chemical dissolution processes rather than firing decomposition. The peculiar and dynamic environment of the Palù di Livenza wetland, characterized by its ponds and watercourses, may have contributed to the dissolution of carbonate inclusions. This interpretation is supported by the lack of reaction rims (Fig. 6g-h), typically formed at high temperatures due to the interaction between coarse carbonate inclusions and the surrounding fired clay (Gliozzo 2020). Additionally, the detection of clay minerals/phyllosilicates is consistent with relatively low firing temperatures and available data on Neolithic pottery technology in north-east Italy and the surrounding areas (e.g. Spataro 1999; Žibrat Gašparič 2004; Bernardini et al. 2016; Bernardini et al. 2024) support this conclusion. In summary, the presence of calcite ghosts without reaction rims, the detection of clay minerals/phyllosilicates, and current knowledge of Neolithic technology indicate that firing temperatures did not exceed 700°C (Gliozzo 2020).

Furthermore, similar taphonomic processes have been previously identified at the nearby Neolithic site of Sammardenchia, also situated in the Friulian plain. There, fabric group 2 displays numerous calcite ghosts, resulting from the secondary dissolution of euhedral calcite temper due to environmental conditions (Carbonetto et al. 2009; Fabbri et al. 2014).

Taphonomic processes may have also altered the original composition of the clay matrix, making comparisons with potential natural sources difficult. The chemical analysis shows a very low CaO content in all samples (between 0.93 and 1.85 wt%; Table S1), suggesting the use of non-calcareous clay; however, this could be due to the dissolution of very fine-grained carbonate components. Additionally, our chemical knowledge of potential clayey natural sources in the investigated area is limited, further complicating reliable provenance determination. Prevalent non-calcareous clay is reported from the high Friulian plain (Carbonetto et al. 2009; table 5), but low CaO content also characterizes terra rossa (Spada et al. 2002), a typical residual soil of karst areas such as the Cansiglio plateau, situated immediately north and east of Palù di Livenza.

For all these reasons, petrographic features of the main large lithic inclusions are important and can help to define the sources of the raw materials used to produce the vessels. The original carbonate temper material likely originated from a location nearby to the settlement, as the stratified carbonate rocks form the Cansiglio plateau (Fig. 10, lithologies 16b-c, 17c; Carulli 2006; Zanferrari et al. 2008). Similarly, the source of quartzite, siltite and chert could be found nearby the settlement where a Cenozoic succession composed by heterometric and polygenic conglomerates, sandstones and various fine grained terrigenous sedimentary rocks are exposed (Fig. 10, lithologies 20a-b; Carulli 2006; Zanferrari et al. 2008).

The general chemical pattern similarity of all samples is in agreement with a local origin of the assemblage. This similarity arises from the dissolution of carbonate materials, which, if preserved, would have influenced the composition of fabric groups 1 and 3. Additionally, the majority of the common lithic inclusions in all fabrics consist of quartzite, while igneous and terrigenous rock fragments are so infrequent that they do not significantly affect the chemical composition.

The PCA analysis of reliable elements obtained by pXRF has revealed that, despite the general chemical similarity of the assemblage, some samples belonging to the same chronological phase and typology form clusters, suggesting slight variations in the raw materials and/or recipes used over time. A notable example is provided by the four-spouted vessels PAL9 and PAL12-14, which are plotted very closely to each other in the PCA diagram (Fig. 9). Both spider diagrams of the elements obtained by ICP-OES/MS (Fig. 7) and the PCA of reliable elements obtained by pXRF (Fig. 9) indeed indicate a clear dilution effect due to the variable occurrence of quartz grains in the analysed samples, sometimes associated with the different chronological phases recognised at the site.

From an archaeological perspective, the analyses conducted offer valuable but preliminary insights for culturally interpreting the Palù di Livenza ceramic complex. They also prompt broader reflections on a phase of prehistory in

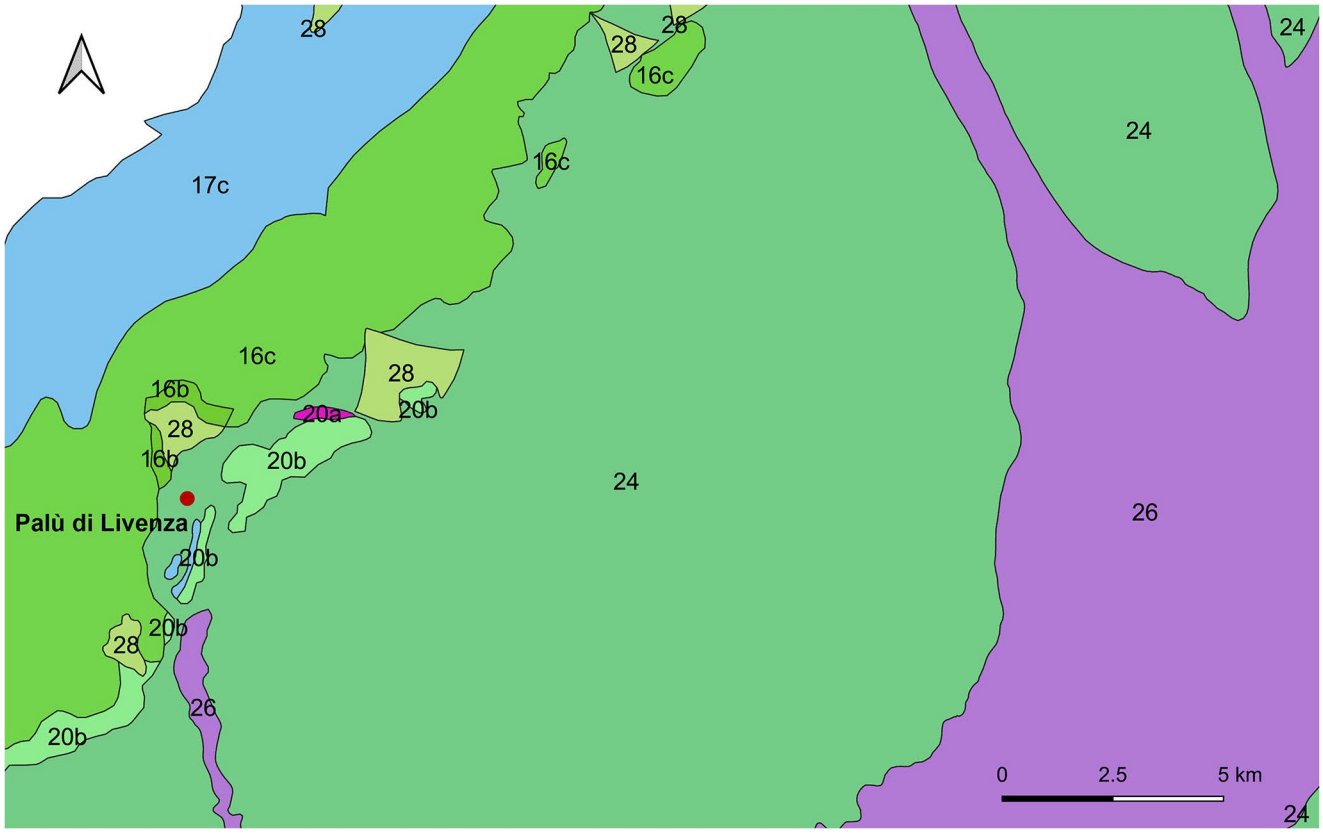

Fig. 10 Geological map of the Palù di Livenza area modified from Carulli 2006. 16b: Micritic limestone and calcarenites; 16c: Well stratified limestones; 17c: Bioclastic massive limestones; 20a: Calcreaous breccias, megabreccias, conglomerates; calcarenites, siltstones and sandstones; conglomerates with carbonate and siliceous metamorphic pebbles; glauconitic sandstones; 20b: Grey silty marls; interbedded sandstones and grey siltstones; polygenic conglomerates; 24: Fluvio-glacial and alluvial sediments of the alluvial plain; 26: Mountain, plain and littoral alluvial sediments; 28: Recent scree slope deposits

north-east Italy, which, as outlined in the introduction, still presents numerous unresolved questions.

The identification of three fabric groups in use throughout the entire duration of the settlement seems to suggest that no significant technological changes occurred at the transition between the end of the SMP culture and the emergence of the earliest Late Neolithic groups.

Another aspect worth considering is how vessels were produced. Micro CT analysis and the macroscopic observation of the Palù pottery assemblage show that some pots, such as PAL6 (Fig. 2), were put together from separately crafted parts characterised by different pastes. This suggests a structured *chaine operatoire*, where various parts of the vessels were likely crafted separately. It indicates that different potters might have been responsible for shaping different components or the possibility that a single individual crafted all parts but not simultaneously. This discovery opens up new perspectives for understanding how ceramics were made during the transition from the Recent to the Late Neolithic periods.

Moreover, it is noteworthy to discuss the vessel fragment PAL8 associated with the Late Hvar culture, distributed in the eastern Adriatic. Since the earliest stages of the Neolithic period, north-east Italy, particularly the Friuli Venezia Giulia region, has documented interactions with cultures from this area (Ferrari et al. 2018), potentially influencing also the evolution of the SMP culture (Visentini 2018, 23–33). This is evident from ceramic materials resembling the Danilo facies, discovered at Sammardenchia, a Friulian site active for approximately a millennium north-west of Udine (Ferrari et al. 2019).

Our findings offer new perspectives on the dynamics of these longstanding interactions, which trace back to the Early Neolithic (Ferrari et al. 2019). They imply more than just the importation of vessels (which often contained the real exchanged commodity); rather, they suggest the transmission of skills or preferences. This is supported by the probable local production of vessel PAL8.

Finally, the validation of pXRF results through comparison with ICP-EOS/MS data has confirmed that this non-destructive, relatively fast, and cost-effective technique can be successfully applied to the chemical characterization of pottery samples, making it a viable alternative to other non-destructive but less flexible archaeometric techniques.

Supplementary Information The online version contains supplementary material available at https://doi.org/10.1007/s12520-024-02043-z.

Acknowledgements This research was funded by Assegnazioni Dipartimentali per la Ricerca–AdiR and Fondo scavi of Ca' Foscari Venezia.

Author contributions FB designed and led the study; RM, PV and FB wrote the introduction and the archaeological background; FB and PV wrote the archaeological part of the conclusions; PV, SR and MP wrote the description of pottery assemblage; FB, MV, ADM and NB wrote all the other parts of the paper; all authors reviewed the manuscript.

Data availability The data that supports the findings of this study are all included within this article.

Declarations

Competing interests The authors declare no competing interests.

References

Al-Musawi M, Kaczmarek S (2020) A new carbonate-specific quantification procedure for determining elemental concentrations from portable energy-dispersive X-ray fluorescence (PXRF) data. Appl Geochem 113. https://doi.org/10.1016/j.apgeochem.2019.104491]. :104491 [DOI

Albero Santacreu D (2014) Materiality, Techniques and Society in pottery production. Current perspectives in the Technological Study of Archaeological Ceramics through Paste Analysis. De Gruyter Open Ltd, Warsaw, Berlin

Barago N, Pavoni E, Floreani F, Crosera M, Adami G, Lenaz D, Larese Filon F, Covelli S (2022) Portable X-ray fluorescence (pXRF) as a Tool for Environmental Characterisation and Management of Mining Wastes: benefits and limits. Appl Sci 12:12189DOI. https://doi.org/10.3390/app122312189

Berg I (2008) Looking through pots: recent advances in ceramics XradiographyJ. Archaeol Sci 35:1177–1188. https://doi.org/10.1016/j.jas.2007.08.006

Bernardini F, Sgambati A, Montagnari Kokelj M, Zaccaria C, Micheli R, Fragiacomo A, Tiussi C, Dreossi D, Tuniz C, De Min A (2013) Airborne LiDAR application to karst areas: the example of Trieste Province (North-Eastern Italy) from prehistoric sites to roman forts. J Archaeol Sci 40:2152–2160

Bernardini F, Vinci G, Horvat J, De Min A, Forte E, Furlani S, Lenaz D, Pipan M, Zhao W, Sgambati A, Potleca M, Micheli R, Fragiacomo A, Tuniz C (2015) Early roman military fortifications and the origin of Trieste (Italy). Proc Natl Acad Sci U S A 112:1520–1529

Bernardini F, Vecchiet A, De Min A, Lenaz D, Mendoza Cuevas A, Gianoncelli A, Dreossi D, Tuniz C (2016) Neolithic pottery from the Trieste Karst (Northeastern Italy): a multi-analytical study. Microchem J 124:600–607

Bernardini F, Leghissa E, Prokop D et al (2019) X-ray computed microtomography of late copper age decorated bowls with cross-shaped foots from central Slovenia and the Trieste Karst (North-Eastern Italy): technology and paste characterisation. Archaeol Anthropol Sci 11:4711–4728. https://doi.org/10.1007/s12520-019-00811-w

Bernardini F, Vaccari L, Zannini F, Bassetti M, Degasperi N, Rottoli M, Micheli R (2023) Production and use of birch bark tar at the neolithic pile-dwelling of Palù Di Livenza (North-Eastern Italy) revealed by X-ray computed micro-tomography and synchrotron Fourier-transform infrared spectroscopy. Archaeometry 65(4):897–907. https://doi.org/10.1111/arcm.12847

Bernardini F, Montagnari Kokelj M, Velicogna M, Barago N, Lenaz D, De Min A, Leghissa E (2024) Continuity and Innovation in pottery technology: the Karst Region (North-East Italy) from neolithic to early bronze age. Heritage 7(6):2959–2983. https://doi.org/10.3390/heritage7060139

Caloi I, Bernardini F (2024) Revealing primary forming techniques in wheel-made ceramics with X-ray microCT. J. Archaeol Sci. https://doi.org/10.1016/j.jas.2024.106025

Carbonetto S, Lenaz D, Princivalle F (2009) Analisi Chimico-Fisiche dei reperti ceramici provenienti dal sito neolitico di Sammardenchia (Pozzuolo Del Friuli, Ud) e loro confronto con i campioni di suolo ivi raccolti. Gortania 30:51–72

Carulli GB (2006) Note illustrative Carta Geologica Del Friuli Venezia Giulia. scala 1:150.000. Regione Autonoma Friuli-Venezia Giulia. Università Degli Studi Di Trieste, Dipartimento Di Scienze Geologiche, Ambientali E Marine; Università Degli Studi Di Udine. Dipartimento di Georisorse e Territorio, Selca, Firenze

Corti P, Martinelli N, Micheli R, Montagnari Kokelj E, Petrucci G, Riedel A, Rottoli M, Visentini P, Vitri S (1998) Siti umidi tardo-neolitici: nuovi dati da Palù di Livenza (Friuli-Venezia Giulia, Italia). In XIII International Congress of Prehistoric and Protohistoric Sciences (Forlì, 8th-14th September 1996) vol. 6, tomo II. A.B.A.C.O. editions, Forlì, pp 1379–1391

Corti P, Martinelli N, Rottoli M, Tinazzi O, Vitri S (2002) Nuovi dati sulle strutture lignee del Palù di Livenza. In Preistoria e Protostoria del Trentino Alto Adige /Südtirol, Proceedings of the XXXIII Conference of the Istituto Italiano di Preistoria e Protostoria (Trento, 21st-24th October 1997). Istituto di Preistoria e Protostoria, Firenze, pp 293–303

Fabbri B, Gualtieri S, Shoval S (2014) The presence of calcite in archeological ceramics. Journal of the European Ceramic Society 34(7)1899–1911.

Ferrari A, Forenbaher S, Micheli R, Montagnari Kokelj M, Pessina A, Velušček A, Visentini P (2018) Neolithic and copper age. In: Borgna E, Càssola Guida P, Corazza S (eds) Preistoria E Protostoria Del Caput Adriae (Atti della XLIX Riunione Scientifica dell'IIPP). Studi Di Preistoria E Protostoria. Istituto Italiano di Preistoria e Protostoria, Firenze, pp 61–74

Ferrari A, Forenbaher S, Pessina A, Podrug E, Roma S, Visentini P (2019) Contatti e interazioni nel Neolitico tra il Friuli e Adriatico orientale. In Atti del Convegno … le quistioni nostre paletnologiche più importanti… Trent'anni di tutela e ricerca preistorica in Emilia occidentale, 8–9 giugno 2017. Parma, pp 171–182

Forenbaher S, Kaiser T, Miracle P (2013) Dating the East Adriatic Neolithic. Eur J Archaeol 16(4):589–609

Gait J, Bajnok K, Szilágyi V et al (2022) Quantitative 3D orientation analysis of particles and voids to differentiate hand-built pottery forming techniques using X-ray microtomography and neutron tomography. Archaeol Anthropol Sci 14:223. https://doi.org/10.1007/s12520-022-01688-y

Gliozzo E (2020) Ceramic technology. How to reconstruct the firing process. Archaeol Anthropol Sci 12:260. https://doi.org/10.1007/s12520-020-01133-y

Gosselain OP, Livingstone-Smith A (2005) The source: clay selection and processing practices in Sub-saharan Africa. In: Smith AL, Bosquet D, Martineau R (eds) Pottery Manufacturing processes: Reconstruction and Interpretation. BAR International Series, vol 1349. Archaeo, Oxford, pp 33–47

Govindaraju K, Mevelle G (1987) Fully automated dissolution and separation methods for inductively coupled plasma atomic emission spectrometry rock analysis. Application to the determination of rare earth elements. J Anal at Spectrom 2:615–621. https://doi.org/10.1039/ja9870200615

JCPDS–International Centre for Diffraction Data (1993) Mineral Powder Diffraction file: search manual: sets 1–42. International Centre for Diffraction Data
Kahl W-A, Ramminger B (2012) Non-destructive fabric analysis of prehistoric pottery using high-resolution X-ray microtomography: a pilot study on the late mesolithic to neolithic site Hamburg-Boberg. J Archaeol Sci 39:2206–2219
Lemière B (2018) A review of pXRF (field portable X-ray fluorescence) applications for applied geochemistry. J Geochem Explor 188:350–363. https://doi.org/10.1016/j.gexplo.2018.02.006
Lindahl A, Pikirayi I (2010) Ceramics and change: an overview of pottery production techniques in northern South Africa and eastern Zimbabwe during the first and second millennium AD. Archaeol Anthropol Sci 2:133–149
Machado AS, Oliveira DF, Gama Filho HS, Latini R, Bellido AVB, Assis JT, Anjosb MJ, Lopes RT (2017) Archeological ceramic artifacts characterization through computed microtomography and X-ray fluorescence. X-Ray Spectrom 46:427–434. https://doi.org/10.1002/xrs.2786
Marijanović B (2005) Gudnja - višeslojno prapovijesno nalazište. Dubrovački muzeji, Dubrovnik
Micheli R (2018) Abitare le aree umide della pedemontana veneto-friulana alla fine del Neolitico: nuovi dati dal Palù di Livenza. In Arnosti G, Riviera G, Schincariol F (eds), Dalla preistoria all'Alto medioevo nell'Antico Cenedese, Antichità Altoadriatiche 89:75–96
Micheli R, Bassetti M, Degasperi N (2017) Le nuove ricerche al Palù di Livenza, sito palafitticolo preistorico. In Micheli R (ed), Il Palù di Livenza e le palafitte del sito UNESCO: nuovi studi e ricerche, Pagine dall'ecomuseo 17 - Percorso acqua:75–85
Micheli R, Bassetti M, Degasperi N, Fozzati L, Martinelli N, Rottoli M (2018) Nuove Ricerche Al Palù Di Livenza: lo Scavo Del Settore 3. In: Borgna E, Cassola Guida P, Corazza S (eds) Preistoria E Protostoria Del Caput Adriae. Istituto di Preistoria e Protostoria, Firenze, pp 481–490
Micheli R, Bassetti M, Degasperi N (2022) Fondamenta. Costruire sull'acqua al Palù di Livenza. In Asta A, Capulli M (eds) Per aquam ad astra. Studi di archeologia delle acque in onore di Luigi Fozzati. Mantova, pp 191–206
Micheli R, Bassetti M, Degasperi N (2023) Palù di Livenza: un insediamento pluristratificato del Neolitico nella Pedemontana pordenonese. In Caramella L A R (ed) Dall'acqua alla terra: cambiamenti nell'occupazione del territorio, Sibrium – Atti 1. Varese, pp 26–61
Mottes E, Petrucci G, Rottoli M, Visentini P (2011) Evolution of square mouthed pottery culture in Trentino Alto Adige, Veneto and Friuli: Cultural, Chronological, Palaeoeconomics and Environmental aspects. Gortania. Geologia, Paleontologia. Paletnologia 31:97–124
Pedregosa F et al (2011) Scikit-learn: machine learning in Python. J Mach Learn Res 12:2825–2830
Rice PM (2015) Pottery analysis: a sourcebook (second edition). University of Chicago Press
Ross P-S, Bourke A, Fresia B (2014) Improving lithological discrimination in exploration drill-cores using portable X-ray fluorescence measurements: (1) testing three Olympus Innov-X analysers on unprepared cores. Geochem Explor Environ Anal 14:171–185. https://doi.org/10.1144/geochem2012-163
Rouillon M, Taylor MP (2016) Canfield portable X-ray fluorescence (pXRF) produce high quality data for application in environmental contamination research? Environ Pollut Barking Essex 1987 214:255–264. https://doi.org/10.1016/j.envpol.2016.03.055
Roux V (2017) Ceramic manufacture: the chaîne opératoire approach. In: Hunt AMW (ed) The Oxford handbook of archaeological ceramic analysis. Oxford University Press, Oxford, pp 101–114
Roux V (2019) Ceramics and society: a technological approach to archaeological assemblages. Springer, Cham
Rudnick RL, Gao S (2004) Composition of continental crust. In: H D Holland, K K Turekian (eds), Treatise on Geochemistry (Vol. 3 (The Crust)). Elsevier, pp 1–64
Rye OS (1981) Pottery technology: principles and reconstruction. Taraxacum, Washington
Sanger MC (2016) Investigating pottery vessel manufacturing techniques using radiographic imaging and computed tomography: studies from the late archaic American southeast. J Archaeol Sci Rep 9:586–598
Shuttleworth EL, Evans MG, Hutchinson SM, Rothwell JJ (2014) Assessment of lead contamination in Peatlands using Field Portable XRF. Water Air Soil Pollut 225:1844. https://doi.org/10.1007/s11270-013-1844-2
Spada P, Lenaz D, Longo Salvador G, De Min A (2002) Mappa Geochimica preliminare dei suoli di dolina del Carso triestino: analisi geo-statistica e implicazioni genetiche. Mem Soc Geol It 57:569–575
Spataro M (1999) La Caverna Dell'Edera Di Aurisina (TS): archeometria delle ceramiche. Atti Soc. Preist. Protost. Reg. Friuli-Venezia Giulia 11:63–90
Tasca G, Bassetti M, Degasperi N, Salvador S, Micheli R (2019) Piastra Di cottura dal sito palafitticolo neolitico di Palù Di Livenza (PN). IpoTESI Di Preistoria 12:17–26
Thér R (2020) Ceramic technology. How to reconstruct and describe pottery-forming practices. Archaeol Anthropol Sci 12:172. https://doi.org/10.1007/s12520-020-01131-0
Tuniz C et al (2013) The ICTP-Elettra X-ray laboratory for cultural heritage and archaeology. Nuclear instruments and methods in Physics Research. Sect A 711:106–110
US EPA (1998) Environmental Technology Verification Report, Field Portable X-ray Fluorescence Analyzer. Metorex X-MET 920-P. United States Environmental Protection Agency. EPA/600/R-97/146
Visentini P (2018) La fine del neolitico nell'Italia nord-orientale. Insediamenti E produzioni tra V e IV millennio a.C. / the end of the neolithic in North-Eastern Italy. Settlement and Productions between 5th and 4th millennium BC. MILLENNI, vol 15. Museo e Istituto Fiorentino di Preistoria, Firenze
Vitri S, Visentini P (eds) (2002) Il Palù alle sorgenti del Livenza: ricerca archeologica e tutela ambientale, Proceedings of the conference (Polcenigo, 16th April 1999). Roveredo in Piano (PN)
Vitri S, Martinelli N, Čufar K (2002) Dati cronologici dal sito di Palù di Livenza. In Ferrari A, Visentini P (eds) Il declino del mondo neolitico. Ricerche in Italia centro-settentrionale fra aspetti peninsulari, occidentali e nord-alpini, Proceedings of the conference (Pordenone, 5th-7th April 2001). Pordenone, pp 187–198
Whitbread IK (1986) The characterisation of argillaceous inclusions in ceramic thin sections. Archaeometry 28:79–88. https://doi.org/10.1111/j.1475-4754.1986.tb00376.x
Whitbread IK (2016) Fabric description of Archaeological ceramics. In: Alice MW Hunt (ed) The Oxford Handbook of Archaeological Ceramics Analysis. Oxford University Press, pp 200–216
Woods AJ (1985) An introductory note on the use of tangential thin sections for distinguishing between wheel-thrown and coil/ring-built vessels. Bull Exp Firing Group 3:100–114
Zanferrari A, Avigliano R, Grandesso P, Monegato G, Paiero G, Poli ME, Stefani C (2008) Note illustrative della Carta Geologica d'Italia alla scala 1:50.000 - Foglio 065 Maniago. APAT-Servizio Geologico d'Italia - Regione Autonoma Friuli- Venezia Giulia. Arti Grafiche Friulane, Udine
Zappa J, Degasperi N, Bassetti M, Florenzano A, Torri P, Servera-Vives G, Mercuri AM, Micheli R (2023) Plants, Fire and Landscape at the prehistoric pile-Dwelling Village of Palù Di Livenza

(PaluON1), UNESCO Site in the Italian Alps. Quaternary 6(2):34. https://doi.org/10.3390/quat6020034
Žibrat Gašparič A (2004) Archaeometrical analysis of neolithic pottery from the Divaca region, Slovenia. Doc Praehistorica 31:205–220